Journal of Solid Mechanics and Materials Engineering

Vol. 4, No. 8, 2010

Thermal Stress and Heat Transfer Coefficient for Ceramics Stalk Having Protuberance Dipping into Molten Metal*

Nao-Aki NODA**, Hendra**, Wenbin LI**, Yasushi TAKASE**,
Hiroki OGURA** and Yusuke HIGASHI**

** Department of Mechanical Engineering, Kyushu Institute of Technology
Sensui-Cho 1-1 Tobata-Ku, Kitakyushu-Shi, Fukuoka, Japan
E-mail: noda@mech.kyutech.ac.jp

Abstract

Low pressure die casting is defined as a net shape casting technology in which the molten metal is injected at high speeds and pressure into a metallic die. The low pressure die casting process plays an increasingly important role in the foundry industry as a low-cost and high-efficiency precision forming technique. In the low pressure die casting process is that the permanent die and filling systems are placed over the furnace containing the molten alloy. The filling of the cavity is obtained by forcing the molten metal, by means of a pressurized gas, to rise into a ceramic tube having protuberance, which connects the die to the furnace. The ceramics tube, called stalk, has high temperature resistance and high corrosion resistance. However, attention should be paid to the thermal stress when the stalk having protuberance is dipped into the molten aluminum. It is important to reduce the risk of fracture that may happen due to the thermal stresses. In this paper, thermo-fluid analysis is performed to calculate surface heat transfer coefficient. The finite element method is applied to calculate the thermal stresses when the stalk having protuberance is dipped into the crucible with varying dipping speeds. It is found that the stalk with or without protuberance should be dipped into the crucible slowly to reduce the thermal stress.

Key words: Thermal Stress, Ceramics Stalk, Low Pressure Die Casting Machine, Protuberance, FEM

1. Introduction

Generally, structural engineering ceramics are widely used in all kinds of engineering fields for their advantages of high temperature resistance, corrosion resistance and abrasion resistance. The ceramics material has been used for auto heat engine, gas turbine, stalk in the low pressure die casting machine as shown in Fig.1 (a), and roll in the galvanizing line (see Fig. 1 (b)). Low pressure die casting machine (LPDC) is especially suitable for producing axi-symmetric component such as cylinder head, piston, and brake drum [(1),(2)]. Ceramic tube called stalk has been used in the LPDC. Stalk has high temperature resistance and high corrosion resistance. Previously, the stalk was made of cast iron which resulted in spoiling the quality of the product due to the partial melting of molten metal. Therefore, ceramics stalk was introduced to improve the life time of tube. However, there is still low reliability of ceramics mainly due to low fracture toughness.

*Received 16 Nov., 2009 (No. e84-2)
[DOI: 10.1299/jmmp.4.1198]

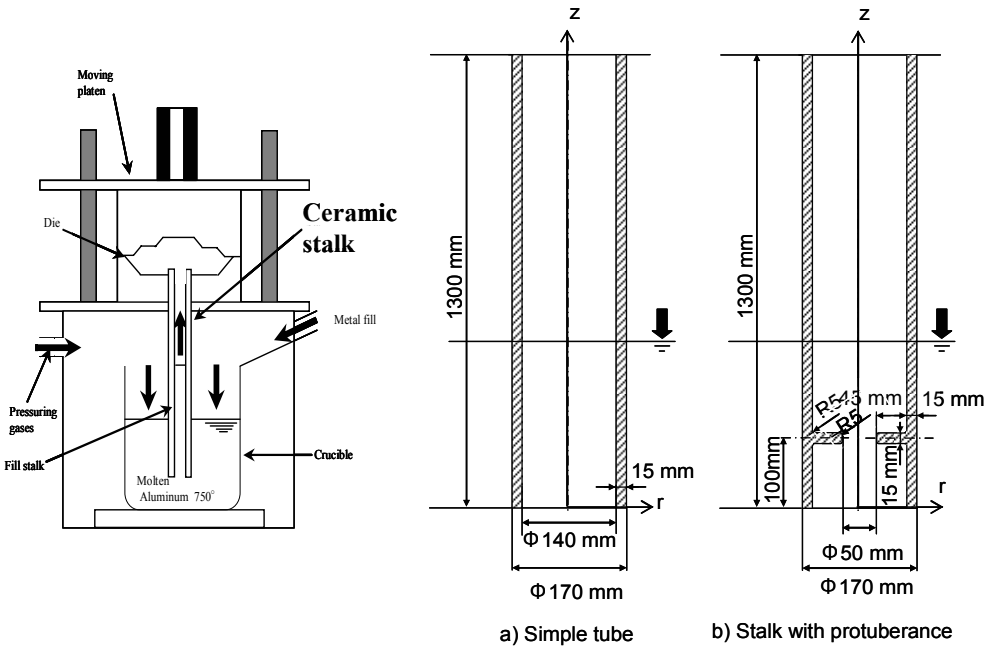

Fig. 1 (a) Schema of the low pressure die casting (LPDC) machine
(Note that LPDC is sometimes called "low pressure casting" in Japan)

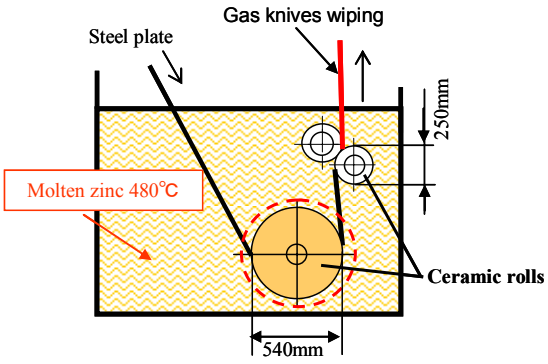

Fig. 1 (b) Zinc bath in the galvanizing line

The ceramic stalk plays a critical function in the LPDC because it receives the molten metal with high temperature from the crucible. However, attention should be paid to the thermal stress when the ceramics stalk is dipped into the molten metal. It is important to reduce the risk of fracture because of low fracture toughness of ceramics. In this paper the finite volume method is applied to calculate surface heat transfer coefficient. Then, the finite element method is applied to calculate the thermal stresses when the stalk having protuberance is dipped into the crucible with varying dipping speeds. Figure 1 (a) shows the model of ceramics stalk for simple model and stalk with protuberance.

2. Effect of Heat Transfer Coefficient on Thermal Stress when Ceramic Dipping into Molten Metal

In this paper, we consider a new thermal stress problem when ceramics cylinder is dipping into molten metal. In this problem, since the value of heat transfer coefficient α is not well known, first, we will check the effect of α on the thermal stress of ceramics. Here, we consider a simple two-dimensional (2D) circular model in Fig. 3 (a) to investigate the effect of heat transfer coefficient on the thermal stress because Zukauskas [3] proposed a

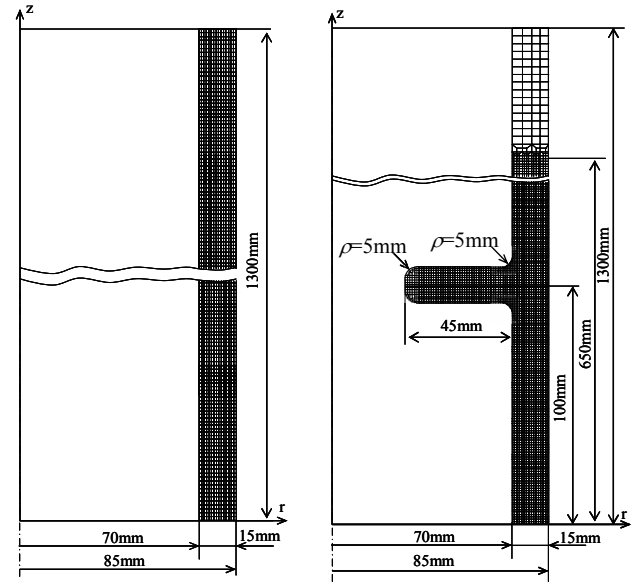

Fig. 2 Finite element mesh of ceramics stalk
(Note that the protuberance has the radius $\rho = 5\text{mm}$)

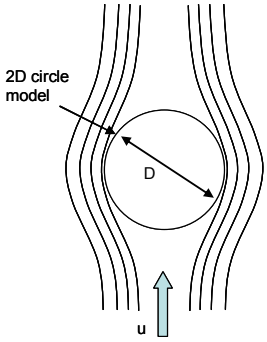

Fig. 3 (a) 2D circle model

convenient formula to estimate heat transfer coefficient for 2D circle (see Eq.1 in Sec. 3.2).

In this paper, three values of α are assumed for boundary conditions in the finite element method analysis, first $\alpha_{Zu} = 6.348\times10^{3}\,\text{W/m}^2\cdot\text{K}$ by Zukauskas formula [4),(5)], second $\alpha_{\max} = 10\times10^{7}\,\text{W/m}^2\cdot\text{K}$ as a very large value of α, and third $\alpha_{FVM} = (2.886-10.214)\times10^{3}\,\text{W/m}^2\cdot\text{K}$ given by applying finite volume method (see Fig.5 (c) in Sec. 3.2). Temperature of the molten aluminum is assumed to be 750^0C (1023K) (see Table 1 in Sec. 3.1), and the initial temperature of the 2D circular model is assumed to be 20^oC. Sialon is used for 2D circular model (see Table 2 in Sec. 3.1) which has total of 510 elements and 548 nodes. The results are shown in Figs. 3 (b) and 3 (c).

From Fig. 3 (c), it is found that the maximum stress $\sigma_{r\max} = 192\text{MPa}$ at $t = 75\text{s}$ when $\alpha_{Zu} = 6.348\times10^{3}\,\text{W/m}^2\cdot\text{K}$. For this case maximum stress is reached in a long time and the value is smaller than the case of the very large α. Figure 4 (a) shows the temperature distribution and maximum stress by Zukauskas formula. The maximum stress

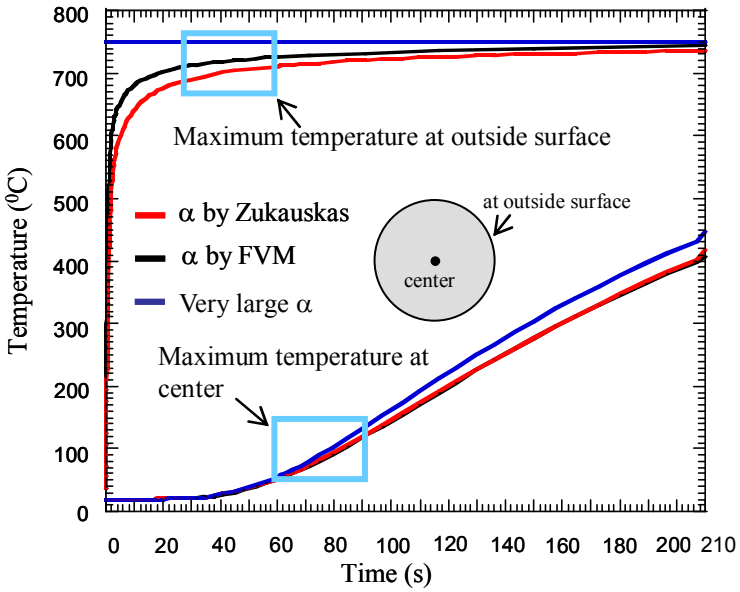

Fig. 3 (b) Maximum temperature vs. time relation of 2D model ($u = 25\text{mm/s}$)

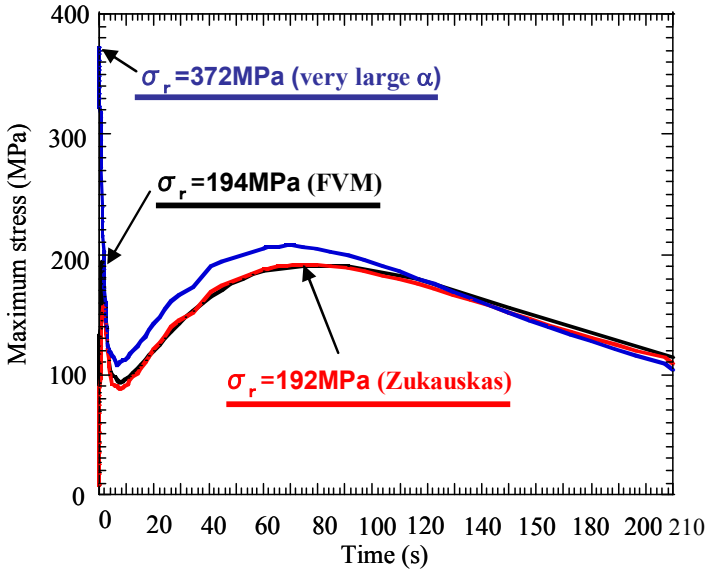

Fig. 3 (c) Maximum stress vs. time relation of 2D model ($u = 25\text{mm/s}$)

appears at the center of circle as shown in Fig. 4 (a).

Utilizing the large value of α, it is found that maximum stress $\sigma_{r\max} = 372\text{MPa}$ appears at $t = 0.01\text{s}$ when $\alpha_{\max} = 10\times10^{7}\,\text{W/m}^2\cdot\text{K}$. For this case the maximum stress is reached to be the large value in a short time. Figure 4 (b) shows the temperature distribution and maximum stress for the large α. As shown in Fig. 4 (b), the maximum stress appears near surface. This is due to the large temperature difference appearing near outside surface very shortly.

Figure 3 (c) shows maximum stress by finite volume method calculation, $\sigma_{r\max} = 194\text{MPa}$ at $t = 0.98\text{s}$ when $\alpha_{FVM} = (2.886-10.214)\times10^{3}\,\text{W/m}^2\cdot\text{K}$ (see Fig. 5 (c)). The time to reach the maximum stress is shorter than the Zukauskas formula although the value is almost the same. Figure 4 (c) shows the temperature distribution and maximum stress by finite volume method. As shown in Fig. 4 (c), the maximum stress appears near

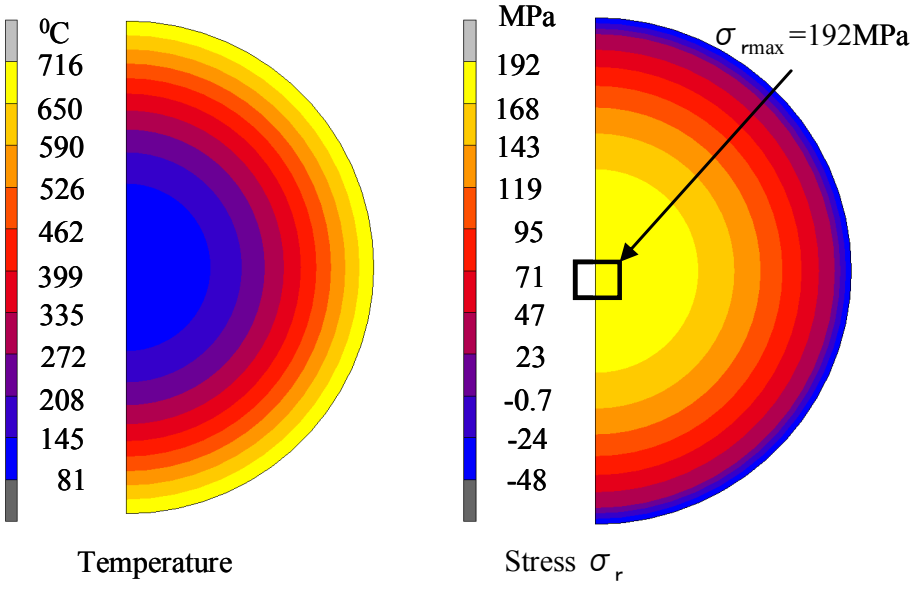

Fig. 4 (a) Temperature and stress distribution for 2D model by Zukauskas formula ($u = 25\text{mm/s}$, $t = 75\text{s}$)

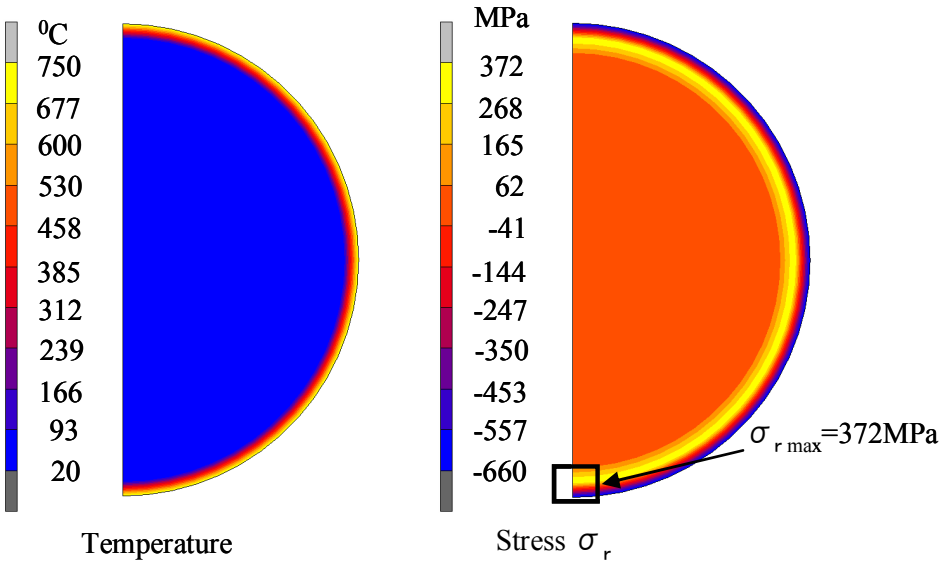

Fig. 4 (b) Temperature and stress distribution for 2D model by very large α ($u = 25$mm/s, $t = 0.01$s)

the surface at the bottom of circle. This is due to the large temperature difference appearing near the surface at the bottom of circle.

As shown in Fig. 3 (c), the maximum stress due to the very large α is larger than that due to Zukauskas formula and finite volume method. From the above discussion, it is found that just assuming a very large α does not provide correct thermal stresses. Maximum stress of α using Zukauskas formula and FVM is nearly the same, but the time for reaching maximum stress is different. It may be therefore concluded that the finite volume method is desirable for calculating thermal stress of ceramics correctly.

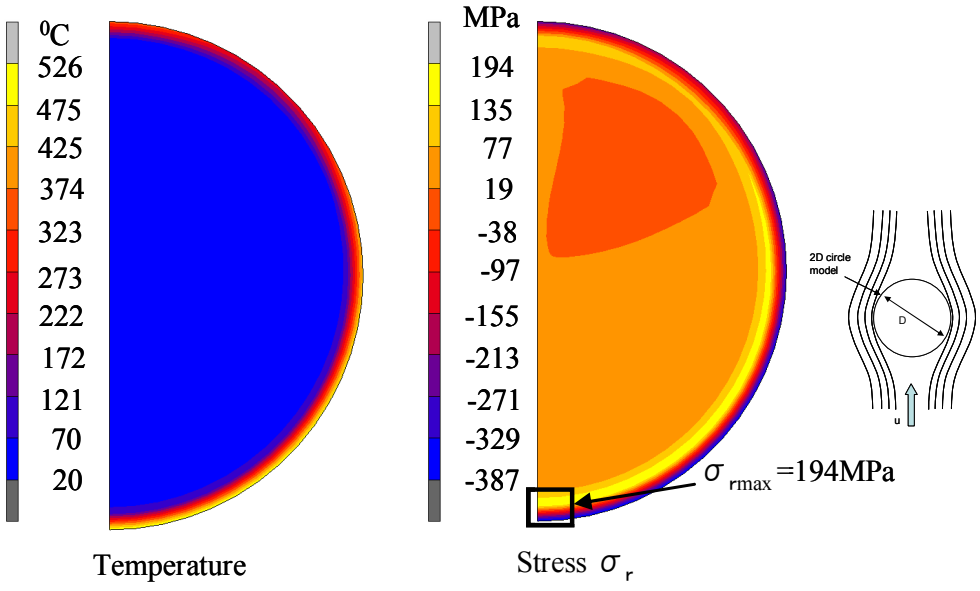

Fig. 4 (c) Temperature and stress distribution for 2D model by finite volume method ($u = 25$mm/s, $t = 0.98$s)

Table 1 The Physical properties of molten aluminum at 750°C (1023K)

Physical property (dimension)	
Thermal conductivity λ, W/m K	112.2
Roll diameter D, m	0.17
Kinematics viscosity ν, mm^2/s	0.967
Isobaric specific heat C_p, kJ/kg K	1.1
Viscosity η, mPa s	2.2
Constants in Eq. (1) when $Re = 1\times10^3 - 2\times10^5$ (C_1)	0.26
Constants in Eq. (1) when $Re = 1\times10^3 - 2\times10^5$ (n)	0.6

Table 2 Mechanical properties of ceramics

Mechanical properties of ceramics (dimension)	Sialon
Thermal conductivity, W/m K	17
Specific heat, J/kg K	650
Coefficient of linear expansion, 1/K	3.0×10^{-6}
Young's modulus, GPa(kgf/mm^2)	294 (29979)
Specific weight	3.26
Poisson's ratio	0.27
4 Point bending strength, MPa (kgf/mm^2)	1050 (107)
Fracture toughness, MN/m$^{3/2}$	7.5

3. Analysis Method for Surface Heat Transfer Coefficient

3.1 Analysis Model and Material Properties

In low pressure die casting machine, the stalk is 170mm in diameter and 1300 mm in length. As shown in Fig. 1 the stalk has the protuberance with the root radius $\rho = 5$mm. The stalk is made of ceramic because of its high temperature resistance and high corrosion resistance. Temperature of the molten aluminum is assumed to be 750°C, and the initial temperature of the ceramics stalk is assumed to be 20°C. Table 1 shows the physical

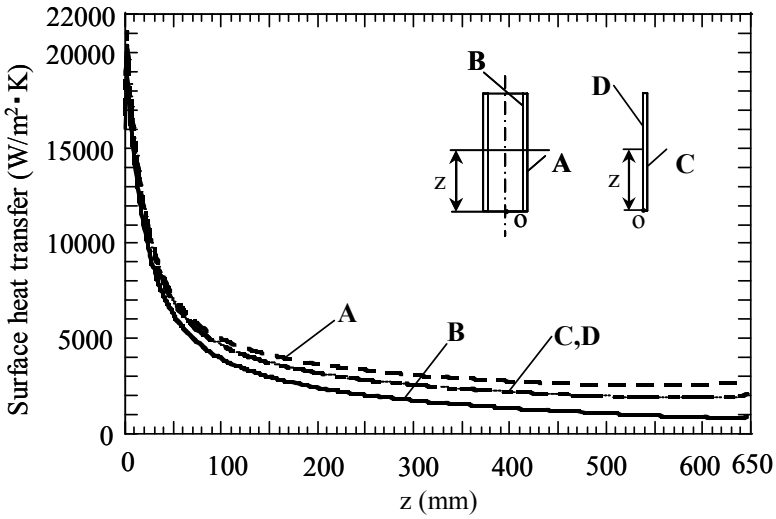

Fig. 5 (a) Surface heat transfer coefficient for 2D and axi-symmetry model as a function of z in the molten metal with the velocity $u = 25$mm/s

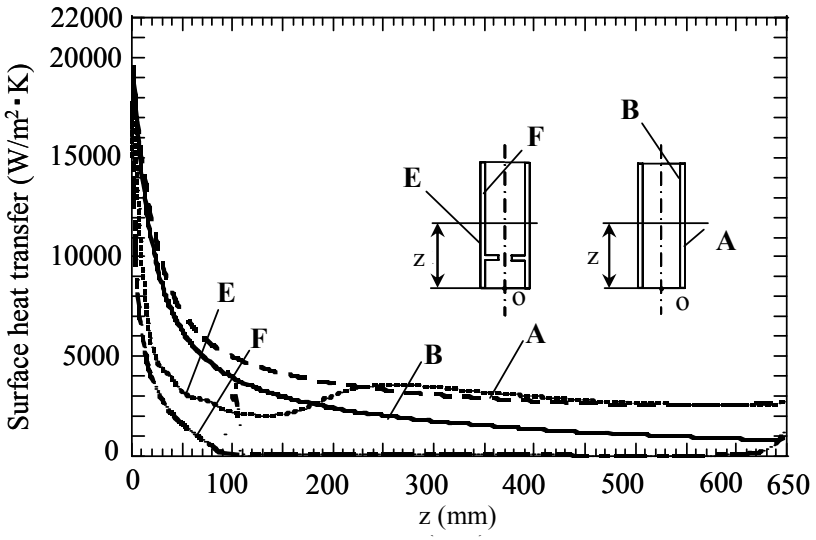

Fig. 5 (b) Surface heat transfer coefficient for simple tube and stalk with protuberance models as a function of z in the molten metal with the velocity $u = 25\text{mm/s}$

properties of molten aluminum at 750°C (1023K) [5]. Table 2 shows the mechanical properties of ceramics called Sialon [4] used for the stalk. Axi-symmetric model will be used for simple tube with a total of 19500 elements and 20816 nodes, and for stalk having protuberance with a total of 14931 elements and 16278 nodes as shown in Fig. 2. In this paper, laminar model [6],[7] is applied for finite volume method and 4-node quadrilateral elements are employed for FEM analysis.

3.2 Surface Heat Transfer Coefficient for Ceramics Stalk

To calculate the thermal stress, it is necessary to know the surface heat transfer coefficient α when the stalk dips into the molten aluminum. In this paper, two-dimensional (2D) and axi-symmetric models are analyzed by using the finite volume method to calculate α when the stalk is dipped into the molten metal. Figure 5(a) shows

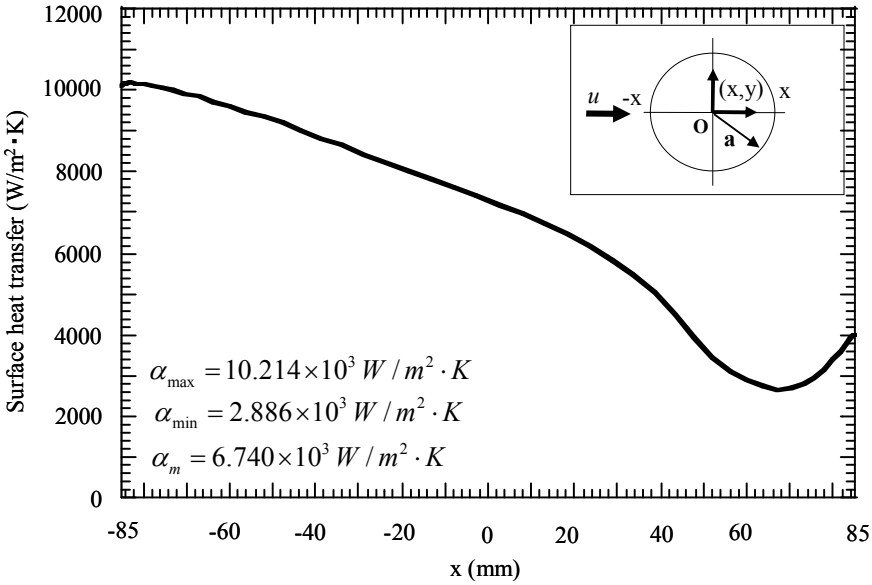

Fig. 5 (c) Surface heat transfer as a function of x for two-dimensional cylinder in the molten metal with the velocity $u = 25\text{mm/s}$

Table 3 surface heat transfer coefficient α, W/m^2.K

Model	Simple model under vertical dipping (Molten Al T=750°C)	Stalk having protuberance model under vertical dipping (Molten Al T=750°C)	Cylinder model under horizontal dipping (Molten Al T=750°C)
	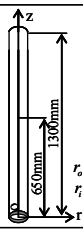 $r_o = 85\text{mm}$ $r_i = 70\text{mm}$	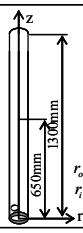 $r_o = 85\text{mm}$ $r_i = 70\text{mm}$	$r_o = 85\text{mm}$ $r_i = 70\text{mm}$ 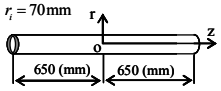
$u = 2\text{mm/s}$	For dipping step by step until reaching half tube: $\alpha = 1.523\times10^3\ \text{W/m}^2\cdot\text{K}$ 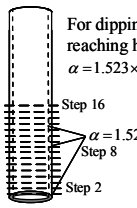 $\alpha = 1.523\times10^3\ \text{W/m}^2\cdot\text{K}$ given	For dipping step by step until reaching half tube: $\alpha = 1.523\times10^3\ \text{W/m}^2\cdot\text{K}$ 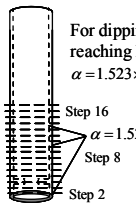 $\alpha = 1.523\times10^3\ \text{W/m}^2\cdot\text{K}$ given	For dipping step by step: $\alpha = 1.523\times10^3\ \text{W/m}^2\cdot\text{K}$ 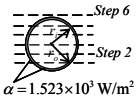 $\alpha = 1.523\times10^3\ \text{W/m}^2\cdot\text{K}$ given
$u = 25\text{mm/s}$	(1) $t = 0$-60s Along outer surfaces $r_o = 85\text{mm}$ $z: 0$-650mm $\alpha = (2.534\text{-}19.105)\times10^3\ \text{W/m}^2\cdot\text{K}$ Along inner surfaces $r_i = 70\text{mm}$ $z: 0$-650mm $\alpha = (0.831\text{-}19.516)\times10^3\ \text{W/m}^2\cdot\text{K}$ For lower end surface $z = 0\text{mm}$ $\alpha = 16.090\times10^3\ \text{W/m}^2\cdot\text{K}$ $\alpha = (0.831\text{-}19.516)\times10^3\ \text{W/m}^2\cdot\text{K}$ $\alpha = (2.534\text{-}19.105)\times10^3\ \text{W/m}^2\cdot\text{K}$ $\alpha = 16.090\times10^3\ \text{W/m}^2\cdot\text{K}$ (2) $t = 60\text{s}$-600s For exposed surface until reaching half tube: $\alpha = 0.831\times10^3\ \text{W/m}^2\cdot\text{K}$ $\alpha = 0.831\times10^3\ \text{W/m}^2\cdot\text{K}$	(1) $t = 0$-60s Along inner and outer surfaces $r_i = 70\text{mm}$ $r_o = 85\text{mm}$ $z: 0$-650mm $\alpha = (0.035\text{-}18.11)\times10^3\ \text{W/m}^2\cdot\text{K}$ For lower end surface $z = 0\text{mm}$ $\alpha = 15.091\times10^3\ \text{W/m}^2\cdot\text{K}$ $\alpha = (0.035\text{-}15.281)\times10^3\ \text{W/m}^2\cdot\text{K}$ $\alpha = (2.527\text{-}18.11)\times10^3\ \text{W/m}^2\cdot\text{K}$ $\alpha = 0.25\times10^3\ \text{W/m}^2\cdot\text{K}$ $\alpha = 0.034\times10^3\ \text{W/m}^2\cdot\text{K}$ $\alpha = 0.25\times10^3\ \text{W/m}^2\cdot\text{K}$ $\alpha = 15.091\times10^3\ \text{W/m}^2\cdot\text{K}$ $\alpha = (2.24\text{-}3.64)\times10^3\ \text{W/m}^2\cdot\text{K}$ $\alpha = 1.130\times10^3\ \text{W/m}^2\cdot\text{K}$ (2) $t = 60\text{s}$-600s For exposed surface until reaching half tube: $\alpha = 0.034\times10^3\ \text{W/m}^2\cdot\text{K}$ $\alpha = 0.034\times10^3\ \text{W/m}^2\cdot\text{K}$	(1) $t = 0$-60s Along outer surfaces $r_o = 85\text{mm}$ $\alpha = (2.886\text{-}10.214)\times10^3\ \text{W/m}^2\cdot\text{K}$ At both ends $z = \pm650\text{mm}$ $\alpha = 2.886\times10^3\ \text{W/m}^2\cdot\text{K}$ Along inner surfaces $r_i = 70\text{mm}$ $\alpha = 2.886\times10^3\ \text{W/m}^2\cdot\text{K}$ $\alpha = 2.886\times10^3\ \text{W/m}^2\cdot\text{K}$  $\alpha = (2.886\text{-}10.214)\times10^3\ \text{W/m}^2\cdot\text{K}$ (2) $t > 60\text{s}$ For all exposed surface: $\alpha = 2.886\times10^3\ \text{W/m}^2\cdot\text{K}$ $\alpha = 2.886\times10^3\ \text{W/m}^2\cdot\text{K}$ 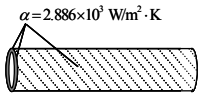

the results of α for the 2D and axi-symmetric models at $u = 25\text{mm/s}$. For axi-symmetric model, the values of the surface heat transfer coefficient α inner (B) and outer (A) of stalk are different as shown in Fig. 5(a). It is confirmed that when the diameter of the axi-symmetric model is infinity the value of α coincides with 2D results. Figure 5(b) shows the surface heat transfer coefficient α of stalk with protuberance compared with the simple tube at $u = 25\text{mm/s}$. As shown in Fig. 5(b) the values of α for inner (F) of stalk with protuberance are much smaller than those of the simple tube (B). The molten metal cannot go into the stalk with protuberance smoothly and most of the molten metal has to detour the tube. Therefore, the outer α of stalk with protuberance is also lower than the outer α of the simple tube when $z < 200\text{mm}$. Table 3 shows the values of surface heat transfer coefficient α for simple tube and for stalk with protuberance at $u = 2\text{mm/s}$ and $u = 25\text{mm/s}$.

In this section, the calculation α for a two-dimensional cylinder using Zukauskas [5] is compared with the finite volume method calculation. Zukauskas [3] proposed the following equation to estimate Nusselt number for a two-dimensional cylinder in the fluid with the velocity u.

$$Nu_m \equiv \frac{\alpha_m \cdot D}{\lambda} = C_1 \cdot Re^n \cdot Pr^{0.37} \cdot \left(\frac{Pr}{Pr_w}\right)^{0.25} \tag{1}$$

$$Re = \frac{u \cdot D}{\nu}, \quad Pr = \frac{C_p \cdot \eta}{\lambda} \tag{2}$$

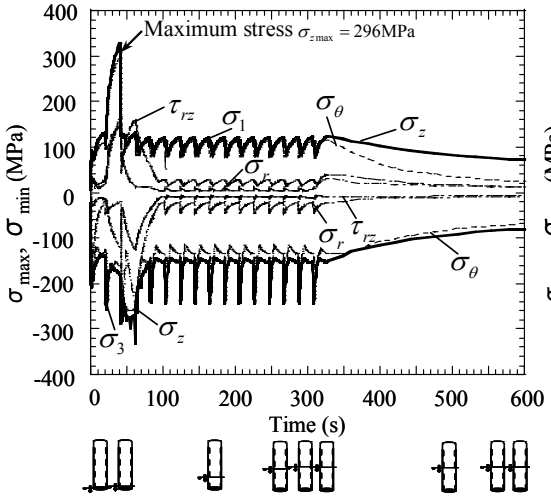

Fig. 6 Maximum stresses vs. time relation for stalk with protuberance ($u = 2$mm/s , figures below the abscissa show the dipping level in the molten aluminum)

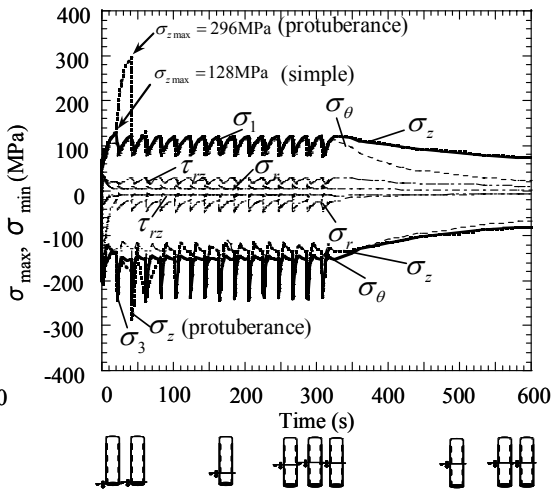

Fig. 7 Maximum stresses vs. time relation for simple model ($u = 2$mm/s , figures below the abscissa show the dipping level in the molten aluminum)

Here, α_m is the average surface heat transfer coefficient, λ is thermal conductivity, D is the diameter of the cylinder, C_1 and n are constants determined by Reynolds number Re. Also, Pr is Prandtl number, and subscript w denotes the property for temperature of cylinder wall. The velocity u can be calculated by the diameter of the tube divided by the time when the tube dips into the molten aluminum, which is usually $u = 2 - 25$mm/s . The values of isobaric specific heat C_p, viscosity η, kinematics viscosity ν are taken from reference [4], as shown in Table 1. Substituting these into Eqs. (1) and (2), Nu_m is calculated for the determination of α_m, which is,

$$\alpha_m = 1.523\times10^3\ \mathrm{W/m^2\cdot K} \quad (\text{when } u = 2\text{mm/s}). \qquad (3)$$

$$\alpha_m = 6.348\times10^3\ \mathrm{W/m^2\cdot K} \quad (\text{when } u = 25\text{mm/s}). \qquad (4)$$

Figure 5 (c) shows the distribution of surface heat transfer coefficient as a function of x for two-dimensional cylinder in the molten metal with the velocity $u = 25$mm/s . The results for $a = 85$mm in molten aluminum are obtained by the application of the finite volume method for two-dimensional cylinder model in the molten metal with the velocity $u = 25$mm/s . The results in Fig. 5 (c) are used in horizontal tubes for calculation of thermal stress. In Fig.5 (c), the average value of $\alpha_m = 6.740\times10^3\ \mathrm{W/m^2\cdot K}$ for $a = 85$mm which is in agreement with Eq. (4).

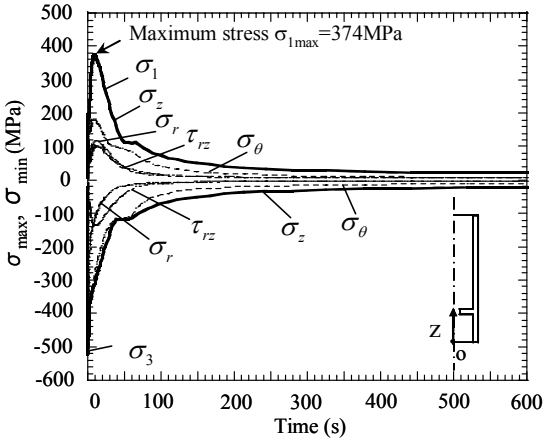

Fig. 8 Maximum stresses vs. time relation for stalk with protuberance ($u = 25$mm/s)

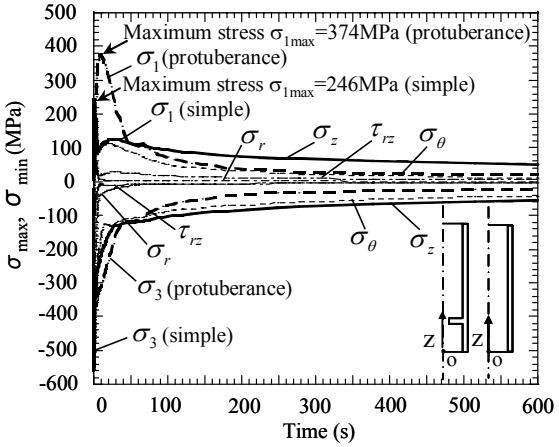

Fig. 9 Maximum stresses vs. time relation for simple model ($u = 25$mm/s)

4. Thermal Stress for Simple Tube and Stalk with Protuberance

The simple tube and stalk having protuberance with the length of 1300mm as shown in Fig.1 is considered when half of the stalk is dipping into molten aluminum at the speeds of $u = 2\text{mm/s}$ and $u = 25\text{mm/s}$. It should be noted that $u < 2\text{mm/s}$ is too slow and not convenient and $u > 25\text{mm/s}$ is too fast and not safe.

4.1 Results for Dipping Slowly

When $u = 2\text{mm/s}$, a constant value $\alpha_m = 1.523\times10^3\,\text{W/m}^2\cdot\text{K}$ is applied for dipping step by step along the inner and outer surfaces ($r_i = 70\text{mm}$ and $r_o = 85\text{mm}$) until reaching half tube. Since it takes 328s for dipping completely, sixteen types of partially dipping models are considered as shown in Table 3, and the value $\alpha_m = 1.523\times10^3\,\text{W/m}^2\cdot\text{K}$ is applied to the whole surface touching molten aluminum. The results are shown in Figs. 6-7. These figures indicate the maximum tensile principle stress σ_1, maximum compressive principle stress σ_3, maximum stresses components σ_r, σ_θ, σ_z and maximum shear stresses τ_{rz}. From Fig. 7 it is seen that $\sigma_{z\max}$ coincides with σ_1 at $t = 20.5\text{s}$ for simple tube. Therefore, only $\sigma_{z\max}$ will be discussed because it is almost equivalent to the maximum stresses σ_1. The stress $\sigma_{z\max}$ ($=\sigma_{1\max}$) has the peak value of 128MPa at $t = 20.5\text{s}$ for simple tube. On the other hand, the maximum stress $\sigma_{1\max}$ ($\cong\sigma_{z\max}$) has the peak value $\sigma_{1\max} = 328\text{MPa}$ ($\sigma_{z\max} = 296\text{MPa}$) at $t = 41\text{s}$ for ceramics stalk with protuberance as shown in Fig. 6. Since the direction of $\sigma_{1\max}$ is not clear, Fig. 6 shows only $\sigma_{z\max}$ because the value and direction of $\sigma_{1\max}$ are close to the ones of $\sigma_{z\max}$.

For simple tube, the maximum stress $\sigma_{z\max} = 128\text{MPa}$ appears at $t = 20.5\text{s}$ and does not decrease while half of the stalk is dipping into molten metal. Then, the stress decreases gradually after half dipping is finished. However, for stalk with protuberance, the maximum stresses $\sigma_{z\max} = 296\text{MPa}$ appears only at $t = 41\text{s}$. After $t = 41\text{s}$ the stress σ_z decreases and coincides with the results for simple tube. Since sixteen types of partially dipping models are utilized, fluctuation of stresses appears as shown in Figs. 6 and 7.

4.2 Results for Dipping Fast

In the previous research [5] the Zukauskas formula was used to calculate heat transfer coefficient for dipping fast for thermal stress analysis. In this paper the finite volume method is used to calculate heat transfer coefficient for thermal stress analysis. The results will be compared with the previous research [5].

Thermal stress is considered when the stalk in Fig. 1 dips into molten aluminum fast at $u = 25\text{mm/s}$. The surface heat transfer is applied as follows (see Table 3):

1. When $t = 0-60\text{s}$, the values in Table 3 $\alpha = (0.831-19.516)\times10^3\,\text{W/m}^2\cdot\text{K}$ is applied at the inner and outer surfaces for simple tube and $\alpha = (0.034-18.11)\times10^3\,\text{W/m}^2\cdot\text{K}$

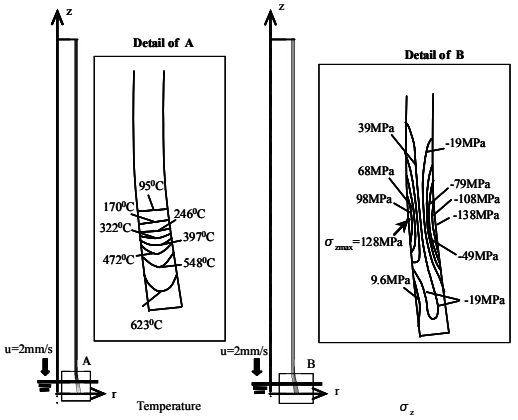

Fig. 10 Temperature and stress distribution for simple model ($u = 2\text{mm/s}$, $t = 20.5\text{s}$) (Bottom parts in the figure show the dipping level in the molten aluminum)

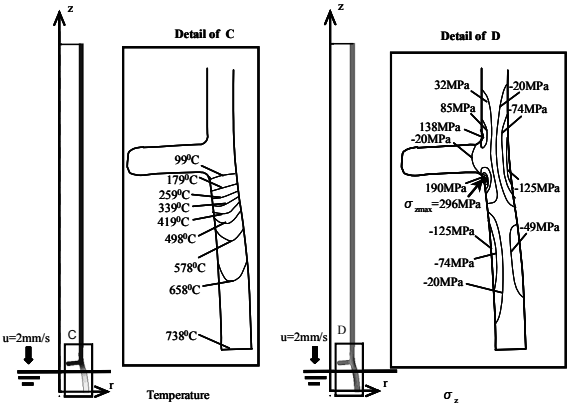

Fig. 11 Temperature and stress distribution for stalk with protuberance ($u = 2\text{mm/s}$, $t = 41\text{s}$) (Bottom parts in the figure show the dipping level in the molten aluminum)

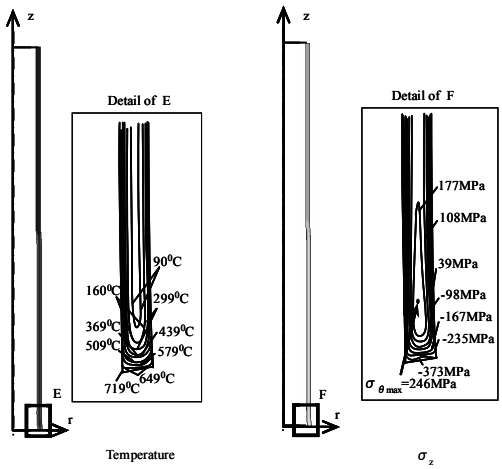

Fig. 12 Temperature and stress σ_θ distributions of vertical tube ($u = 25\text{mm/s}$ at time $t = 1.1\text{s}$), displacement $\times 50$

for stalk with protuberance. Also the maximum value, in Fig. 5 (b), $\alpha = 16.090 \times 10^3\ \text{W/m}^2 \cdot \text{K}$ is applied at the lower end surface ($z = 0\text{mm}$) for simple tube and $\alpha = 15.09 \times 10^3\ \text{W/m}^2 \cdot \text{K}$ for stalk with protuberance.

2. When $t > 60\text{s}$, the minimum value, in Fig. 5 (b) $\alpha = 0.831 \times 10^3\ \text{W/m}^2 \cdot \text{K}$ is applied for the exposed surface until reaching half tube for simple tube and $\alpha = 0.034 \times 10^3\ \text{W/m}^2 \cdot \text{K}$ for stalk with protuberance.

Figures 8 and 9 show the maximum value of stresses σ_1, σ_r, σ_θ, σ_z, τ_{rz}. As shown in Fig. 9, the maximum tensile stress $\sigma_1 = \sigma_\theta$ increases in a short time. After taking a peak value $\sigma_{\theta\max} = 246\text{MPa}$ at $t = 1.1\text{s}$ for simple tube and $\sigma_{1\max} = 374\text{MPa}$ ($\sigma_{z\max} = 363\text{MPa}$) at $t = 8.8\text{s}$ for stalk with protuberance, it is decreasing. The maximum value of stalk with protuberance 374MPa is larger than that of 246MPa for simple tube.

For simple model, the maximum stress for dipping fast by finite volume method is $\sigma_{\theta\max} = 246\text{MPa}$. Comparing this value with the maximum stress previously obtained in Ref. (5) which is $\sigma_{\theta\max} = 219\text{MPa}$. There is 10.9% in difference with the results from finite volume method. For heat transfer coefficient, the maximum α is different by 5%.

4.3 Comparison between Dipping Slowly and Fast

For simple tube, the maximum value $\sigma_{\theta\max} = 246\text{MPa}$ for dipping fast is larger than that of $\sigma_{z\max} = 128\text{MPa}$ for dipping slowly. Similarly, for stalk with protuberance, the

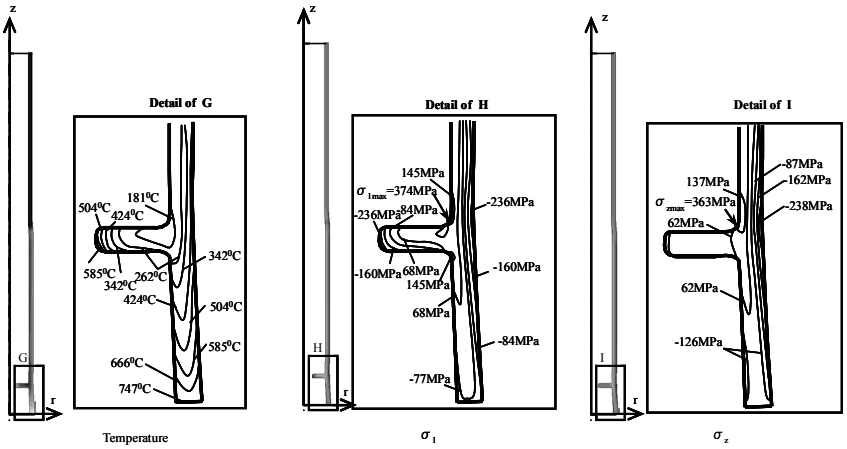

Fig. 13 Temperature and stress σ_z distributions of vertical tube ($u = 2\text{mm/s}$ at time $t = 20.5\text{s}$), displacement $\times 50$

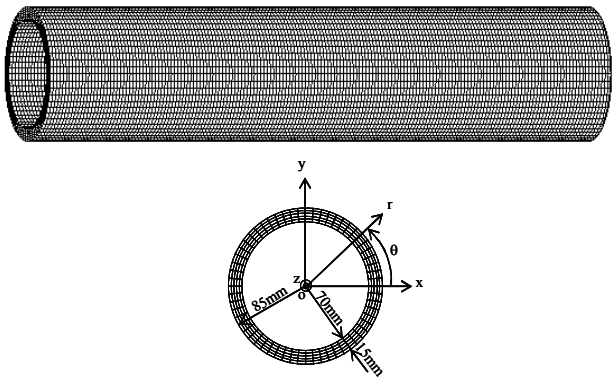

Fig. 14 Finite element mesh of horizontal tube (No. of elements=45000, No. of nodes=55986)

maximum stress $\sigma_{1\max}=374\text{MPa}$ for dipping fast is larger than that of $\sigma_{1\max}=328\text{MPa}$ for dipping slowly. Table 4 shows maximum stresses for stalk with protuberance compared with the results of simple tube at the same time. As shown in Table 4, the maximum value of stalk with protuberance is 2.5 times larger than the value of simple tube at $t=41\text{s}$ for $u=2\text{mm/s}$. On the other hand, for $u=25\text{mm/s}$ the maximum value of stalk with protuberance is 3.6 times larger than the value of simple tube at $t=8.8\text{s}$.

The temperature and stress distributions of simple tube and stalk with protuberance are indicated in Figs. 10-13. Figure 10 shows temperature and stress distributions of σ_z at $t=20.5\text{s}$, where the maximum stress $\sigma_{z\max}=128\text{MPa}$ appears for the simple tube dipping slowly. For dipping slowly at $u=2\text{mm/s}$, the maximum stress σ_z appears at the inner surface of the tube $r=70\text{mm}$ just above the dipping level of molten aluminum as shown in Fig. 10. This is due to the bending moment caused by the thermal expansion of the dipped portion of the tube. Figure 12 shows temperature and stress distributions σ_θ at $t=1.1\text{s}$ where the maximum stress $\sigma_{\theta\max}=246\text{MPa}$ appears for the simple tube dipping fast. For the dipping fast at $u=25\text{mm/s}$, the maximum stress $\sigma_{\theta\max}$ appears on the inside of the thickness as shown in Fig. 12. This is due to the large temperature difference appearing in the thickness direction. It may be concluded that simple tubes should be dipped slowly in order to reduce the thermal stresses.

Figures 11 and 13 show temperature and stress distributions of σ for stalk with protuberance dipping slowly and fast. Figure 11 shows temperature and stress distributions of σ_z at $t=41\text{s}$, where the maximum stress $\sigma_{z\max}=296\text{MPa}$ appears for the stalk with

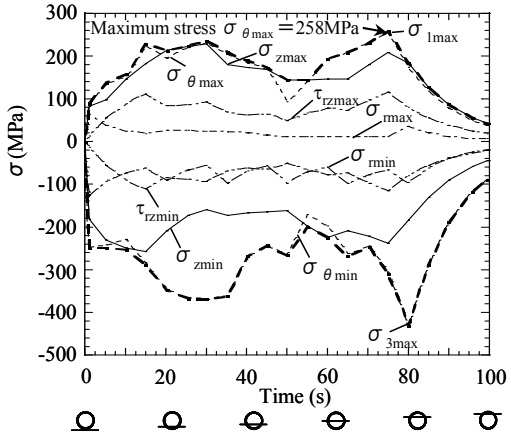

Fig. 15 Maximum stresses vs. time relation for horizontal tube ($u=2\text{mm/s}$, figures below the abscissa show the dipping level in the molten aluminum)

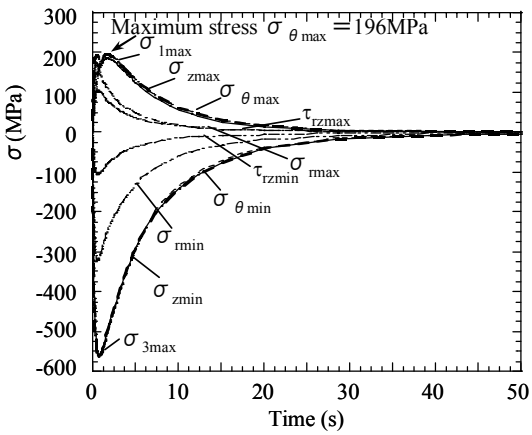

Fig. 16 Maximum stresses vs. time relation for horizontal tube ($u=25\text{mm/s}$)

protuberance dipping slowly. For dipping slowly at $u = 2\text{mm/s}$, the maximum stress σ_z appears at the lower root of the protuberance $\rho = 5\text{mm}$ (see Fig. 11). This is due to the bending moment caused by the thermal expansion of the dipped portion of the tube. Figure 13 shows temperature and stress distributions σ_z at $t = 8.8\text{s}$ where the maximum stress $\sigma_{z\max} = 363\text{MPa}$ appears for stalk with protuberance dipping fast. For the dipping fast at $u = 25\text{mm/s}$, the maximum stress $\sigma_{z\max}$ appears at upper root of protuberance $\rho = 5$ as shown in Fig. 13. This is due to the large temperature difference appearing in the outside the thickness and lower part of stalk.

5. Thermal Stress for Horizontal Tube

Thermal stress is considered when the horizontal tube in Fig. 14 dips into molten aluminum at the speeds of $u = 2\text{mm/s}$ and $u = 25\text{mm/s}$. Three-dimensional model will be used for horizontal tube with a total of 45000 elements and 55986 nodes as shown in Fig. 14.

5.1 Results for Dipping Slowly

When $u = 2\text{mm/s}$, a constant value $\alpha_m = 1.523\times10^3\,\text{W/m}^2\cdot\text{K}$ is applied for dipping step by step along the inner and outer surfaces ($r_i = 70\text{mm}$, $r_o = 85\text{mm}$). Since it takes 210s for dipping completely, six types of partially dipping models are considered as shown in the Table 3, and the value $\alpha_m = 1.523\times10^3\,\text{W/m}^2\cdot\text{K}$ is applied to the surface touching molten aluminum. Figure 15 shows maximum values of stresses σ_1, σ_r, σ_θ, σ_z, τ_{rz}. In Fig. 15, the maximum tensile stress $\sigma_{\theta\max} = 258\text{MPa}$ appears at $t = 75\text{s}$.

5.2 Results for Dipping Fast

Similarly, to the vertical tube dipping fast, the Zukauskas formula was previously used to calculate heat transfer coefficient for horizontal tube dipping fast [5]. In this paper the finite volume method is used to calculate heat transfer coefficient for thermal stress analysis. Then, the results will be compared with the previous research [5].

Thermal stress is considered when the horizontal tube in Fig. 14 dips into the molten aluminum fast at $u = 25\text{mm/s}$. Here, the surface heat transfer is applied in the following way:

1. When $t = 0-60\text{s}$, the values in Table 3 $\alpha = (2.886-10.214)\times10^3\,\text{W/m}^2\cdot\text{K}$ are applied along the outer surface ($r_o = 85\text{mm}$). Also the minimum value in Table 3 $\alpha = 2.886\times10^3\,\text{W/m}^2\cdot\text{K}$ is applied at the inner surface ($r_i = 70\text{mm}$) and tube ends $z = \pm650\text{mm}$.
2. When $t > 60\text{s}$, the minimum value in Table 3 $\alpha = 2.886\times10^3\,\text{W/m}^2\cdot\text{K}$ is applied for all exposed surfaces.

Figure 16 shows maximum values of stresses σ_1, σ_r, σ_θ, σ_z, τ_{rz}. As shown in Fig. 16 the maximum stress increases in a short time, and has a peak value $\sigma_{\theta\max} = 196\text{MPa}$ at

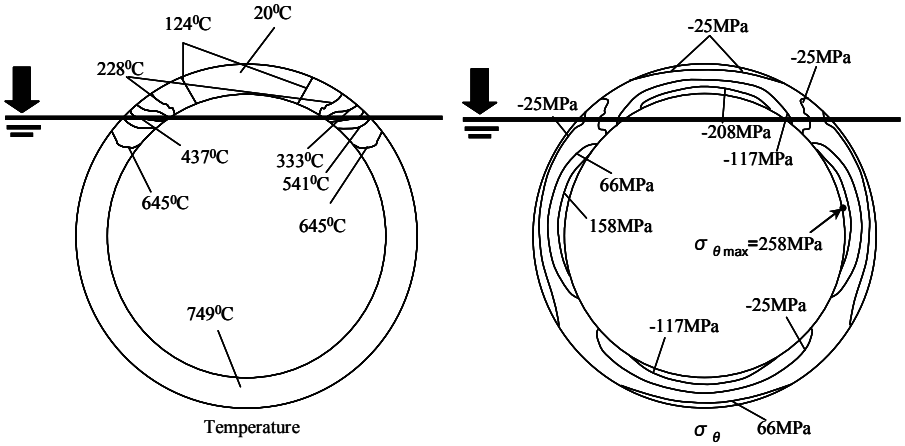

Fig. 17 (a) Temperature and stress σ_θ distributions of horizontal tube at both ends $z = \pm650\text{mm}$ ($u = 2\text{mm/s}$ at time $t = 75\text{s}$)

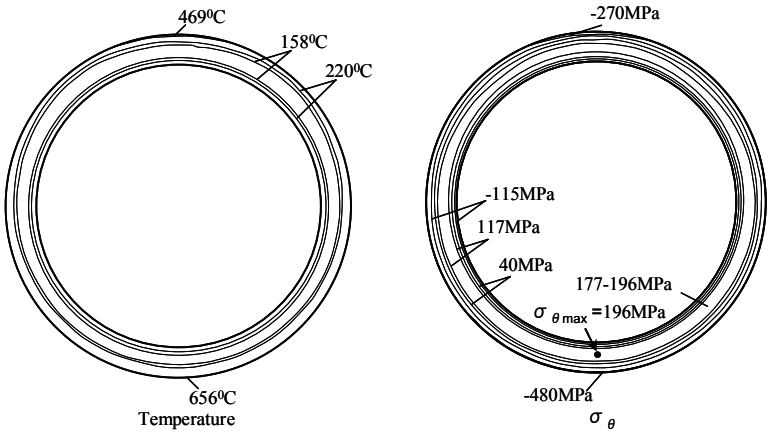

Fig. 17 (b) Temperature and stress σ_θ distributions of horizontal tube near the both ends at $z = 615\text{mm}$ ($u = 25\text{mm/s}$ at time $t = 1.73\text{s}$)

$t = 1.73\text{s}$.

For horizontal tube, the maximum stress for dipping fast by the finite volume method is $\sigma_{\theta\max} = 196\text{MPa}$. Comparing this value with the maximum stress previously obtained in Ref. (5) which is $\sigma_{\theta\max} = 222\text{MPa}$. There is 11% in difference with the results from the finite volume method. For heat transfer coefficient, the maximum α is different by 43%.

5.3 Comparison between Dipping Slowly and Fast

Figure 17 (a) shows the temperature and stress distributions σ_θ for horizontal tube at both ends where $\sigma_{\theta\max} = 258\text{MPa}$ appears at $t = 75\text{s}$ for the tube dipping slowly. Figure 17 (b) shows temperature and stress distributions σ_θ near both ends, where $\sigma_{\theta\max} = 196\text{MPa}$ appears at $t = 1.73\text{s}$ for the tube dipping fast.

For dipping slowly, as shown in Fig. 18 (a) the maximum stress $\sigma_{\theta\max}$ appears at the inner surface of the tube ends $z = \pm 650\text{mm}$. In this case the circular cross section becomes elliptical because of temperature difference between the dipped and upper parts. In other words, the maximum stress $\sigma_{\theta\max}$ appears due to asymmetric deformation. For dipping fast as shown in Fig. 18 (b), the temperature and stress distributions are similar to the ones of vertical tube dipping fast in Fig. 12. In other words, for dipping fast, the deformation is almost axi-symmetric. The larger stress appears much more shortly than the case of $u = 2\text{mm/s}$. Therefore horizontal tubes should dip fast at $u = 25\text{mm/s}$ rather than slowly at $u = 2\text{mm/s}$ to reduce the thermal stress.

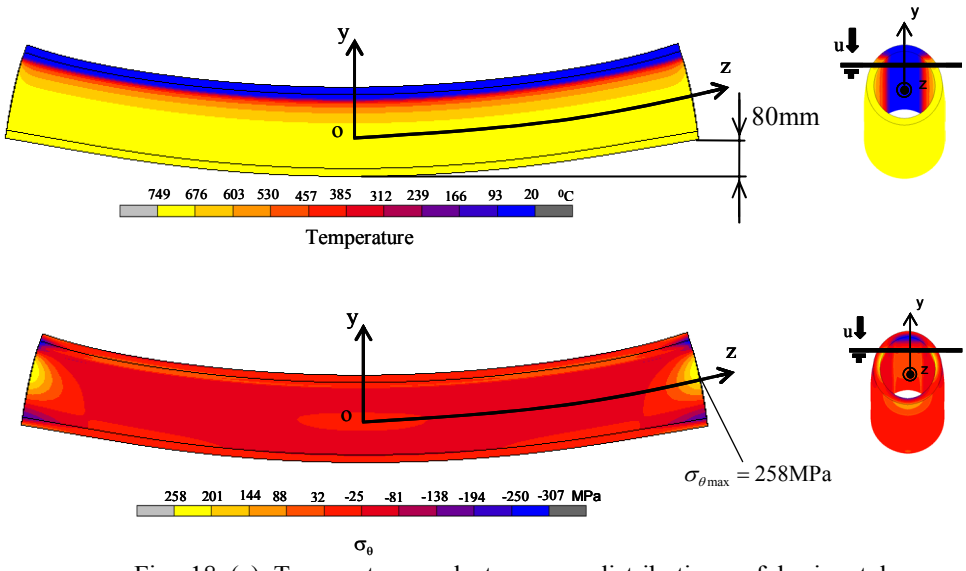

Fig. 18 (a) Temperature and stress σ_θ distributions of horizontal tube ($u = 2\text{mm/s}$ at time $t = 75\text{s}$), displacement×30

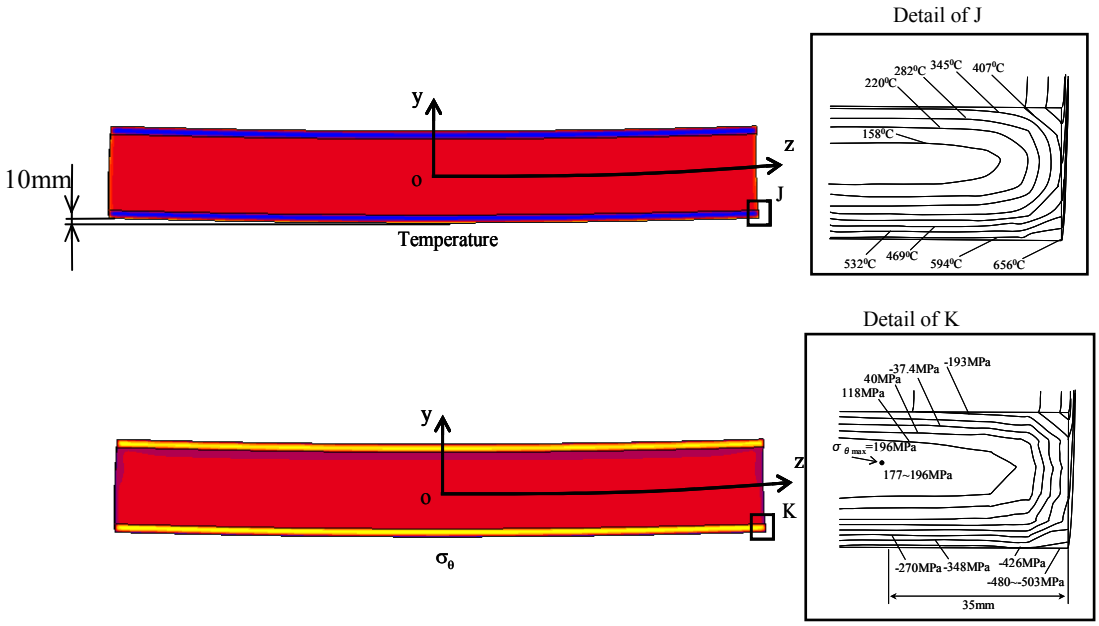

Fig. 18 (b) Temperature and stress σ_θ distributions of horizontal tube ($u = 25$mm/s at time $t = 1.73$s), displacement×30

Table 4 Maximum stresses for stalk with protuberance compared with the results of simple tube at the same time.

	Stalk with protuberance		Simple tube			Horizontal tube
Model						
u=2mm/s	At t=41s (maximum stress appears) $\sigma_1 = 328$MPa (A) $\sigma_z = 296$MPa (A) $\sigma_\theta = 162$MPa (B) $\sigma_r = 167$MPa (A) $\tau_{rz} = 150$MPa (A)	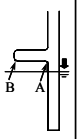	At t=41s $\sigma_1 = 120$MPa (A) $\sigma_z = 120$MPa (A) $\sigma_\theta = 110$MPa (A) $\sigma_r = 4$MPa (A) $\tau_{rz} = 28$MPa (B)	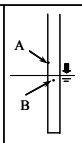	At t=20.5s (maximum stress appears) $\sigma_1 = 128$MPa (A) $\sigma_z = 128$MPa (A) $\sigma_\theta = 105$MPa (B) $\sigma_r = 4$MPa (A) $\tau_{rz} = 21$MPa (C)	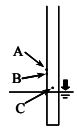	At t=75s (maximum stress appears) $\sigma_1 = 258$MPa $\sigma_\theta = 258$MPa $\sigma_z = 210$MPa $\sigma_r = 11$MPa $\tau_{rz} = 116$MPa
u=25mm/s	At t=8.8s (maximum stress appears) $\sigma_1 = 374$MPa (A) $\sigma_z = 363$MPa (A) $\sigma_\theta = 181$MPa (A) $\sigma_r = 116$MPa (A) $\tau_{rz} = 98$MPa (B)	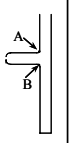	At t=8.8s $\sigma_1 = 101$MPa (A) $\sigma_z = 101$MPa (A) $\sigma_\theta = 97$MPa (A) $\sigma_r = 7$MPa (C) $\tau_{rz} = 18$MPa (B)	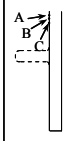	At t=1.1s (maximum stress appears) $\sigma_1 = 246$MPa (A) $\sigma_\theta = 246$MPa (A) $\sigma_z = 209$MPa (A) $\sigma_r = 89$MPa (A) $\tau_{rz} = 98$MPa (B)	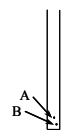	At t=1.73s (maximum stress appears) $\sigma_1 = 196$MPa $\sigma_\theta = 196$MPa $\sigma_z = 186$MPa $\sigma_r = 112$MPa $\tau_{rz} = 80$MPa

5.4 Comparison between the Results of Vertical and Horizontal Tubes

Table 4 shows the maximum values of tensile stresses for simple tube, stalk with protuberance, and horizontal tube. For both simple tube and stalk with protuberance, dipping slowly for ceramics stalk may be suitable for reducing the thermal stresses because dipping fast causes larger temperature difference in the thickness direction, which results in larger thermal stresses. On the other hand, for horizontal tube, dipping fast may reduce the thermal stress although in this case similar large temperature difference appears in the thickness direction. Those different conclusions may be explained in terms of deformations of the tube. For simple tube and stalk with protuberance, the deformation is always axi-symmetric. However, for horizontal tube, dipping slowly causes large asymmetric deformation, which results in the largest $\sigma_{\theta\max}$ at the inner surface of the end of the tube. On the other hand, for fast dipping of horizontal tube, the deformation is almost axi-symmetric.

6. Conclusions

In the recent low pressure die casting machine, the stalk is usually made of ceramics because of high temperature and corrosion resistances. However, attention should be paid to

the thermal stresses when the stalk is dipped into the molten aluminum. In this paper, the finite element method in connection with thermo-fluid analysis using the finite volume method for surface heat transfer coefficient α was applied to calculate the thermal stress when the stalk is installed in the crucible. The conclusions are given as following.

1. Thermal stress for 2D ceramic circle was considered. It was found that accurate α distribution is desirable for obtaining accurate thermal stress by applying the finite volume method (see Figs. 3 and 4).
2. Since the molten metal cannot flow into the stalk with protuberance very much, the inner α of stalk with protuberance is much lower than the inner α of simple tube. Accurate α is shown in Table 3 and Fig. 5 (b).
3. For both simple tube and stalk with protuberance, dipping slowly may be suitable for reducing the thermal stresses because dipping fast causes larger temperature difference in the thickness direction, which results in larger thermal stresses.
4. For horizontal tube, however, dipping fast may be suitable for reducing the thermal stress even though it causes larger temperature difference in the thickness direction of the tube.
5. The different conclusions about the vertical and horizontal tubes may be explained in terms of deformations of tube. For horizontal tube, dipping slowly causes larger asymmetric deformation, which results in larger $\sigma_{\theta\max}$ at the tube ends.

References

(1) "The A to Z of Materials" Aluminum Casting Techniques-Sand Casting and Die Casting Processes. (Online), available from <http://www.azom.com/details.asp? Articled=1392>, (accessed 2008-4-23).

(2) Bonollo, F., Urban, J., Bonatto, B., and Botter, M., Gravity and Low Pressure Die Casting of Aluminium Alloys: a Technical and Economical Benchmark, *Allumino E Leghe*, (2005).

(3) Zukauskas, A., Heat Transfer from Tubes in Cross Flow, In: Hartnett JP, Irvine Jr TF, editors, Advances in Heat Transfer, Vol.8, New York: Academic Press, (1972), p. 131.

(4) Noda, N.A., Yamada, M., Sano, Y., Sugiyama, S., and Kobayashi, S., Thermal Stress for All-ceramics Rolls used in Molten Metal to Produce Stable High Quality Galvanized Steel Sheet, *Engineering Failure Analysis*, Vol. 15, (2008), pp. 261-274.

(5) Noda, N.A., Hendra, Takase, Y., and Li, W., Thermal Stress Analysis for Ceramics Stalk in the Low Pressure Die Casting Machine, *Journal of Solid Mechanics and Material Engineering*, Vol. 3, No.10 (2009), pp. 1090-1100.

(6) Li, H. S, and Mei, C., Thermal Stress in SiC Element used in Heat Exchanger, *Journal Cent. South Univ. Technol.*, Vol. 12, No.6, (2005), pp. 709-713.

(7) Al-Zaharnah, I. T., Yilbas, B. S., and Hashmi, M. S. J., Conjugate Heat Transfer in Fully Developed Laminar Pipe Flow and Thermally Induced Stresses, *Computer Methods in Applied Mechanics and Engineering*, Vol. 190, (2000), pp. 1091-1104.

(8) Editorial committee of JSME, *Data of heat transfer*, Tokyo: JSME, (1986), p.323 [in Japanese].

(9) Korenaga, I., Sialon Ceramics Products used in Molten Aluminum, *Sokeizai* (1991); 5:12-7 [in Japanese].

(10) Nogami, S., Large Sialon Ceramics Product for Structural Use, *Hitachi Metal Report*, Vol.15, (1999), pp.115-120 [in Japanese].

(11) Editorial committee of JSME, *Data of heat transfer*, Tokyo: JSME; (1986), p.61 [in Japanese].